Potassium-limitation of forest productivity, part 2: CASTANEA-MAESPA-K shows a reduction in photosynthesis rather than a stoichiometric limitation of tissue formation

Ivan Cornut[1,2,5], Guerric le Maire[2,5], Jean-Paul Laclau[2,5], Joannès Guillemot[2,4,5], Yann Nouvellon[2,5], and Nicolas Delpierre[1,3]

[1]Université Paris-Saclay, CNRS, AgroParisTech, Ecologie Systématique et Evolution, 91405, Orsay, France.
[2]CIRAD, UMR Eco&Sols, F-34398 Montpellier, France
[3]Institut Universitaire de France (IUF)
[4]Department of Forest Sciences ESALQ, University of São Paulo, Piracicaba, São Paulo, Brazil
[5]Eco&Sols, Univ. Montpellier, CIRAD, INRAe, Institut Agro, IRD, Montpellier, France

Correspondence: Ivan Cornut (ivan.cornut@cirad.fr)

Abstract. Potassium availability constrains forest productivity. Brazilian eucalypt plantations are a good example of the K-limitation of wood production. Here, we built upon a previously described model (CASTANEA-MAESPA-K) and used it to understand whether the simulated decline in C-source under K deficiency was sufficient to explain the K-limitation of wood productivity in Brazilian eucalypt plantations. We developed allocation schemes for both C and K and included into CASTANEA-MAESPA-K. No direct limitations of the C-sink activity, nor direct modifications of the C-allocation by K availability were included in the model. Simulation results show that the model was successful in replicating the observed patterns of wood productivity, growth, NPP limitation by K deficiency. Simulations also show that the response of NPP is not linear with increasing K fertilisation. Simulated stem carbon use and water use efficiencies decreased with decreasing levels of K availability. Simulating a direct stoichiometric limitation of wood productivity, growth, NPP was not necessary to reproduce the observed decline of productivity under K limitation, suggesting that K stoichiometric plasticity could be different than that of N and P. Confirming previous results from the literature, the model simulated an intense recirculation of K in the trees, suggesting that retranslocation processes were essential for tree functioning. Optimal K fertilisation levels calculated by the model were similar to nutritional recommendations currently applied in Brazilian eucalypt plantations, paving the way for validating the model at a larger scale and this approach to develop decision-making tools to improve fertilisation practices.

Keywords

Potassium - Biogeochemistry - nutrient limitation - NPP - eucalypt - Brazil - Biomass

1 Introduction

Fertilisation trials in tropical eucalypt plantations have been conducted over multiple rotations (Laclau et al., 2010; Battie-Laclau et al., 2016; Gazola et al., 2019; Gonçalves, 2000). These experiments have shown that nutrients can strongly affect
20 tree growth in these highly prodctive stands. These nutrient limitations can be explained in part by low nutrient supplies from highly weathered soils, and in part by the large exports of nutrients from plots with trunk wood (every 6-7 years) from the stands. The frequent export of trunk wood in these fast-growing plantations leads to the export of massive amounts of nutrients that are immobilised in wood (Cornut et al., 2021). In commercial plantations this issue is solved through the use of fertilisers (NPK, dolomitic lime and micro-nutrients).

25 Potassium (K) has been identified as the most limiting nutrient for wood productivity in many omission trials (Gonçalves, 2000; Rocha et al., 2019). Potassium nutrition impacts wood growth through different physiological mechanisms that have been reviewed in detail (Sardans and Peñuelas, 2015; Cornut et al., 2021). In brief, K deficiency is known to depress the assimilation of carbon by the plant (C-source processes, Gross Primary Production) as well as the allocation and use of carbon by the plant for growth (C-sink processes, Net Primary Production).

30 The study of the limitation of GPP (C-source) by K deficiency was explored at the stand level in Part 1 of this series of two papers, using a coupled C-H_2O-K mechanistic model (CASTANEA-MAESPA-K). The simulations showed a strong response of GPP to K deficiency. The GPP in the simulated K omission stand was less than half of that in the simulated fertilised stand (Tab.2, Part 1). These results were consistent with previous measurements (Epron et al., 2012) and modelling work (Christina et al., 2018). The strong response of GPP to K availability was due to a reduction in leaf area index and in the photosynthetic
35 capacity per unit area of leaf. The reduction in canopy area was due in part to a slight reduction in leaf production, in part to a decrease in individual leaf area and in part to a strong decrease in leaf lifespan (Fig.4, Part 1). The reduction in photosynthetic capacity of the canopy was associated with the appearance of leaf symptoms in the K-deficient (oK) stand. The impact of symptom area on leaf photosynthetic capacity was sufficient to explain most of the reduction in leaf-scale assimilation in the unfertilized case. A decrease of WUE_{GPP} in the simulated oK stand was also simulated. A sensitivity analysis of the
40 model parameters showed that competition between the organs (trunk, branches, bark and roots) and leaves for K access had an important impact on GPP in the oK stand (the leaf to phloem resorption resistance, $R_{leaf \rightarrow phloem}$, Fig.7 Part 1). This underlined the need for a precise understanding of K circulation and stoichiometry in the plant.

The impact of K deficiency on net primary productivity (NPP) is a widely observed phenomenon in non-planted forests (Tripler et al., 2006; Baribault et al., 2012) and in planted forest omission experiments (Laclau et al., 2010; Battie-Laclau
45 et al., 2016; Gazola et al., 2019). While a negative effect of K deficiency on GPP is well documented, the magnitude of its contribution to the decrease in trunk NPP remains unclear. Potassium deficiency also impacts phloem mobility (Epron et al., 2016; Marschner et al., 1996), as well as the loading and unloading of sugars into and from the phloem (Doman and Geiger, 1979; Cakmak et al., 1994; Dreyer et al., 2017). Furthermore, Various processes have been described that could explain a sink-limitation of tree growth under K deficiency: it could directly impact organ growth by stoichiometric limitation (through
50 its role as an enzyme co-factor for example). Potassium availability also affects cell turgor pressure (Battie-Laclau et al., 2013)

which plays an important role in tissue expansion (Lockhart, 1965; Muller et al., 2011; Pantin et al., 2012). The present paper focuses on the simulation of the relationship between soil K availability and the NPP of all the main tree organs.

The objectives of the present study were to understand:

1. the impact of K deficiency on the NPP of a Brazilian eucalypt stand representative of large areas of commercial eucalypt plantations,

2. whether the influence of K availability on GPP is sufficient to explain the differences in wood productivity between K-fertilised and K-deficient stands,

3. the link between C partitioning and K availability in the plant-soil system,

4. which parts of the K cycle are the most critical to simulate accurately the consequences of K-limitation on wood productivity,

5. if K:C stoichiometry can contribute to explaining the observed patterns of organ NPP.

We have built on the results related to the K-GPP relationship previously obtained. To this end, the C and K allocation schemes of CASTANEA-MAESPA-K were adapted to Brazilian eucalypt stands. The model was evaluated against data obtained in a K fertilisation-omission experiment. To test the hypothesis of sink limitation of wood NPP, the parsimony principle was applied. Since the model did not include any explicit sink-limitation process, if it was able to replicate observed productivity patterns, that meant that C-source limitation was sufficient to explain wood productivity limitation by K deficiency.

2 Methods

2.1 Study site

A split-plot fertilisation trial was installed at the Itatinga experimental station (23°02'49"S and 48°38'17"W, 860 m asl, University of São Paulo-ESALQ). The precipitation was on average 1430 mm year^{-1}, with a drier season between June and September, and the mean annual temperature was 19.3°C. The trial was established on June 2010, for 6 years. The planted clone was a fast growing *Eucalyptus grandis*. The experimental design was described in detail in Battie-Laclau et al. (2014). Six treatments (three fertilisation regimes crossed with two two water regimes) were applied in three blocks. In the present study, we focus on the +K and oK treatments with undisturbed rainfall regime, which consisted in a non-limiting K fertilisation: +K (17.55 gK m^{-2} applied as KCl with 3.3 gP m^{-2}, 200 g m^{-2} of dolomitic lime and trace elements at planting and 12 gN m^{-2} at 3 months of age); and an omission treatment: oK where all fertilisation was applied as in the +K treatment, except K.

The concentrations of N, P and K (as well as Ca and Mg) in the organs (leaves, trunks, branches, and roots) were measured at an annual time step in 8 individuals of each fertilisation treatment and upscaled to the whole stand using allometric relationships. Biomass and nutrient contents were calculated (using upscaling) from inventories, biomass and nutrient concentration measurements performed at 1, 2, 3, 4, 5 and 6 years in each fertilisation treatment. Atmospheric deposition (0.55 gK m^{-2} yr^{-1}) was measured in a nearby experiment from Laclau et al. (2010).

2.2 CASTANEA-MAESPA-K model

CASTANEA-MAESPA-K is a coupled C-H$_2$O-K mechanistic model that simulates forest growth at the stand level. The original CASTANEA model (Dufrêne et al., 2005), generally used to simulate temperate forest stands was adapted to tropical

85   eucalypt plantations. It was merged with the MAESPA model (Duursma and Medlyn, 2012; Christina et al., 2017) since it does not simulate the water-plant-atmosphere hydraulic continuum natively and the assumption of a fixed root depth made by CASTANEA did not hold true in the studied system (Christina et al., 2011). More information on the construction of the CASTANEA-MAESPA-K model can be found in Part 1 of this two part paper.

Here we focused on NPP (for GPP see Cornut et al., submitted), which led to concentrate efforts on the C and K allocation

90   models (Fig.1). All the sub-models (leaf cohorts, external K cycling, uptake) described in Part 1 were re-used albeit sometimes with different parameter values (Tab.S1-2) since the simulated experimental sites were different. New modules simulating the carbon allocation, the availability of K for organ growth and the remobilisation of K from organs were developed for this work and are presented below.
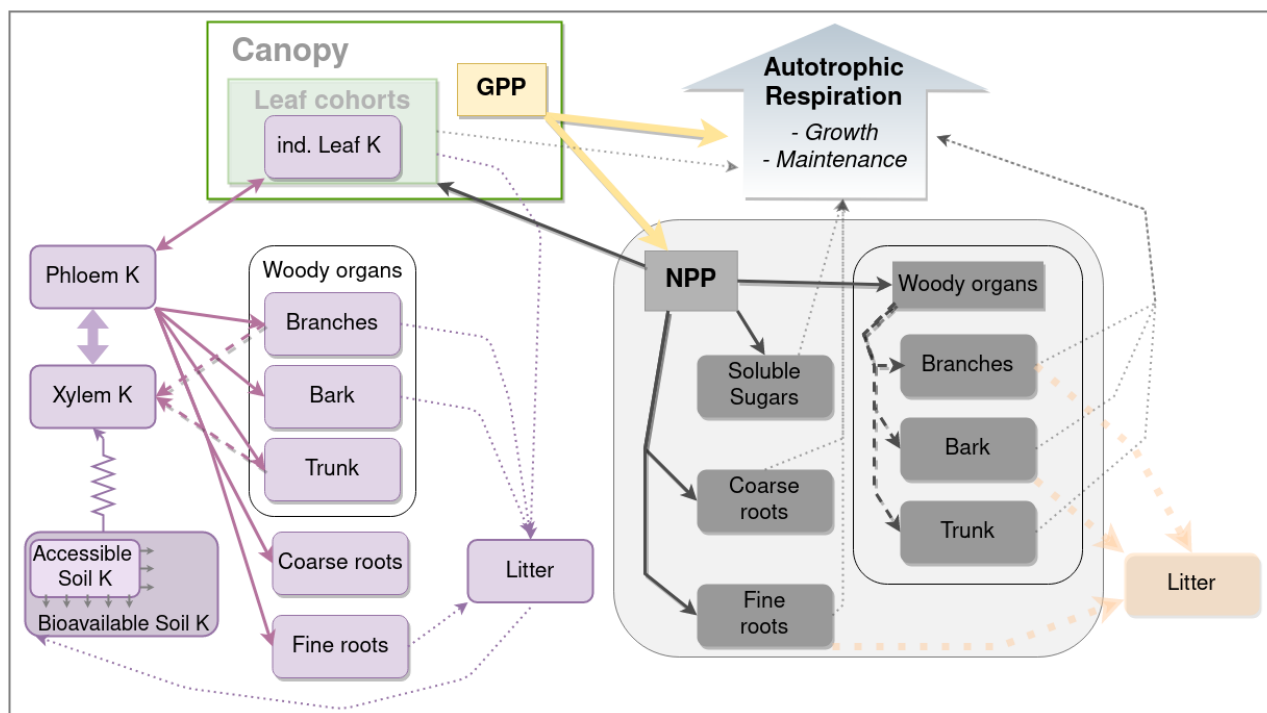
Figure 1. Schematic representation of K balance in the tree, and its link with the allocation model. Purple boxes are K state variables, while purple arrows are K fluxes. Dashed purple arrows are remobilisation fluxes. The K uptake flux simulated with a simple Ohm's law form is represented with resistance symbols. Grey boxes represent C biomasses. Dark grey arrows represent allocation of NPP to the different organs. Thin dotted grey arrows represent the influence of the organ biomass on respiration.

2.3 Carbon allocation

95   In the CASTANEA model, carbon of assimilates was allocated to organ growth and soluble sugars (SSs), after a part of it was released to the atmosphere through maintenance respiration and growth respiration processes. SSs are not localized in the model which, for the carbon part, has no topology. So SSs are hypothesized to be part of the phloem and other tissues, indistinctly. This is different from the K content of the plant, that we localized either in organs or the semi-explicit phloem and xylem saps.

100   The growth of all organs was a fraction of the daily NPP (Fig.1). The allocation coefficients of each organ except leaves (i.e. fine roots, coarse roots, woody organs) were calculated at a daily time-step and were the result of NPP and allometric relationships among organs. The generation of leaves and their growth was a process that was not directly dependent on NPP (see Part 1), and had priority for the allocation of carbon. Leaf growth could however be limited if demand for growth was higher than available C in the SSs compartment.

2.3.1   Leaves

In the model, leaves had carbon priority over other organs. This means that carbon was firstly allocated to leaves and what was left could be allocated to the other organs. Leaf production in the model was driven by the increase in tree height (see Part 1 and eq.8 below). The parameters used here were fitted using experimental data from the +K stand.

2.3.2   Soluble Sugars

110   The optimal biomass of SSs (BSS_{max}) was a function of woody organ biomass (eq. S1). The parameters of the function relating optimal SS biomass to woody organ biomass assumed in a range of realistic values since no data was available on SS content. The allocation coefficient to SSs with a target value corresponding to this optimal biomass was calculated as:

$$G_{SS} = max\left(0, GSS_{max} \times min\left(1, (1 - \frac{B_{SS}}{BSS_{max}}) \times \frac{1}{p_{SS}}\right)\right) \tag{1}$$

where G_{SS} was the (daily) allocation coefficient of soluble sugars, B_{SS} (gC m^{-2}) the biomass of soluble sugars, BSS_{max}

115   (gC m^{-2}) the optimal biomass of soluble sugars and p_{SS} the sensitivity of the response of the allocation coefficient to soluble sugar deficiency.

2.3.3   Roots

In accordance with experiment evidence in the fertilisation experiments, the allocation coefficient of coarse roots was set to a constant:

120   $G_{CR} = 0.01$ $\tag{2}$

The allocation coefficient of carbon to fine roots was similar to Marsden et al. (2013). It used a target function, where the fine root target biomass was a function of leaf area index:

$$G_{FR} = min\left(1 - G_{CR} - G_{SS}, max\left(0, 0.5 \times min\left(1, (1 - \frac{B_{FR}}{\lambda \times L}) \times \frac{1}{p_{FR}}\right)\right)\right) \tag{3}$$

where G_{FR} was the allocation coefficient to fine roots, G_{CR} and G_{SS} the allocation coefficients of coarse roots (eq. 2) and
125 SSs (eq. 1) respectively, B_{FR} (gC.m^{-2}) the fine root biomass, λ (gC.m_{leaf}^{-2}) the conversion coefficient between leaf area and target root biomass, L (m_{leaf}^{2}.m_{soil}^{-2}) the leaf area index of the stand and p_{FR} a sensitivity parameter.

2.3.4 Woody organs

The remaining C available after allocation of NPP to leaves, roots and SSs was allocated to the woody organs (trunk, branches and bark):

130 $$G_W = max(0, 1 - G_{FR} - G_{CR} - G_{SS}) \tag{4}$$

where G_W was the allocation coefficient to woody organs, and G_{FR}, G_{CR} and G_{SS} the allocation to fine roots (eq. 3), coarse roots (eq. 2) and soluble sugars (eq. 1), respectively.

The C allocated to woody organs was then distributed to the different woody organs (trunk, branches and bark) using allometric relationships.

135 Parameters of the function linking the allocation of woody NPP to branches in function of total woody biomass were fitted on experimental data. The following equation was used in the model:

$$G_{Br} = 0.437 \times e^{-0.00240 \times (B_{trunk} + B_{Br} + B_{bark})} + 0.102 \tag{5}$$

where G_{Br} was the ratio of woody NPP allocated to branch production, B_{trunk}, B_{Br}, B_{bark} the biomasses (gC.m^{-2}) of the trunk, branches and bark respectively.

140 Following experimental data, the allocation of woody NPP to bark was considered to be constant:

$$G_{Bark} = 0.10 \tag{6}$$

All the C remaining after allocation of woody NPP to the bark and the branches was used for trunk wood production.

$$G_{trunk} = 1 - G_{Bark} - G_{Br} \tag{7}$$

where G_{Bark} was from eq.6 and G_{Br} from eq.5.

145 The increase in height was a function of trunk biomass. The relationship was fitted in the +K stand using biomass and inventory data (Fig.S1):

$$H = 22.67 \times (1. - e^{-0.00029 \times B_{trunk}})^{0.4989} + 1 \tag{8}$$

where H (m) was the height of the stand and B_{trunk} (gC.m^{-2}) the biomass of the trunk.

2.4 Autotrophic Respiration fluxes

150 ### 2.4.1 Growth respiration

Each organ in the model had an associated construction cost. The growth respiration was calculated as in Dufrêne et al. (2005), from the growth of the considered organ and its construction cost.

2.4.2 Maintenance respiration

The hourly maintenance respiration for all organs (except leaves which had a respiration rate based on their vertical position
155 in the canopy, Christina et al., 2015) was a function of their respective respiration rate per nitrogen unit (see below), nitrogen content and surface temperature (Dufrêne et al., 2005).

Firstly the respiration rates per unit nitrogen were calculated. For the trunk, we used data from Ryan et al. (2009) to calculate the maintenance respiration rate per unit nitrogen, as a function of trunk biomass:

$$MRN_{Trunk} = max\left[0.00047, \, 0.0073 - 1.16 \times 10^{-6}\right] \times B_{Trunk} \times 10^{-6} \times 3600 \times \frac{1}{12} \times \frac{1}{N_{trunk}} \quad (9)$$

160 where MRN_{Trunk} (mol $CO_2.gN^{-1}.hr^{-1}$) was the respiration rate of the trunk per nitrogen unit, B_{trunk} the trunk biomass in $gC.m^{-2}$, 3600 the number of seconds per hour, 12, the molar mass of carbon and N_{Trunk} the concentration of N per unit mass of trunk ($gN.gC^{-1}$). The respiration rate per nitrogen unit of roots (MRN_R) and branches (MRN_{Br}) was assumed to be equal to twice MRN_{Trunk}.

The N content of roots was fixed at 0.0050 $gN.gC^{-1}$ since no variation was visible in the experimental data. The N content of
165 branches and trunks was a decreasing exponential function of their respective biomasses that was calibrated using experimental data (Fig.S2):

$$N_{branches} = min\left(0.5, 0.256 \times e^{-0.00966*B_{branches}} + 0.2604\right) \times 0.005$$
$$N_{trunk} = min\left(0.5, 0.256 \times e^{-0.00854*B_{trunk}} + 0.0759\right) \times 0.005 \quad (10)$$

where $N_{branches}$ and N_{trunk} were the respective N concentrations ($gN.gC^{-1}$) of the branches and the trunk, and $B_{branches}$, B_{trunk} the respective biomasses ($gC.m^{-2}$) of the branches and the trunk. The N content of leaves and bark were not simulated
170 since N content did not influence the respiration of leaves in our model and bark had no maintenance respiration.

Following Dufrêne et al. (2005), the maintenance respiration of an organ (except leaves, see below) was:

$$RM_{organ} = B_{organ} \times MRN_{organ} \times N_{organ} \times Q_{10}^{(T_{org}-T_{MR})/10} \quad (11)$$

where RM_{organ} ($CO_2.hr^{-1}$) was the respiration rate of the organ, B_{organ} (gC) the biomass of the organ, MRN_{organ} the respiration rate per unit nitrogen ($CO_2.gN^{-1}.hr^{-1}$, eq. 9), N_{organ} ($gN.gC^{-1}$) the N concentration of the organ, and Q_{10} the
175 exponential relationship between the respiration rates and temperature.

The maintenance respiration of leaves was their dark respiration (inhibited during the day), Rd, and the values measured in K-fertilised trees in a nearby site (Eucflux) were used (see Part 1).

2.5 Organ turnover

With the exception of the coarse roots and the trunk, the organs (branches, bark, fine roots) were subject to turnover. Branches,
180 bark, fine roots and leaves each had lifespans.

In simulations, the theoretical (independently of K limitation effects) leaf lifespan (LLS) was considered to be constant
throughout the rotation. This option was chosen since we were unable to mechanistically model the observed variations in leaf
lifespan. The realised lifespan of leaves was influenced by their K status (see Part 1). We assumed that the lifespans of bark
($BarkLS$, Fig.S3b), branches ($BrLS$, Fig.S3a) and fine roots ($FRLS$, Lambais et al. (2017)) depended neither on tree age
185 nor on the nutritional status of the organs.

The necromass of most organs was added to the litter pool. On the other hand, dead branches were added to the the dead
branch pool. The dead branch pool represented the branches that stay attached to the tree after senescence. The dead branch
pool had a specific turnover rate.

Resorption of K took place during the senescence of leaves (see Part 1) and branches (Fig.S4a). K remobilised from these
190 two organs was added to the phloem sap K pool. While the resorption rate for leaves was dependent on the nutritional status of
the tree and their theoretical lifespan, for branches it was fixed.

2.6 K allocation, remobilisation and turnover

The allocation of K to organs was a function of the optimal K concentration of newly formed organ tissue, organ NPP and K
availability in the tree. Firstly, organ NPP was calculated by allocating part of GPP to the organs after subtracting the respiration.
195 Then, the total K quantity required was calculated by multiplying the growth of each organ by its optimal K concentration (the
concentration of newly formed organs in the fully fertilised stand). If the quantity of available K in the phloem sap was inferior
to the demand, K allocation to the organs was limited without affecting C allocation to the organ's growth. This was equivalent
to flexivle stoichiometry in other models.

$$K_{NPP} = NPP_{org} \times \left([K]_{wood}^{opti} \times G_{trunk} + [K]_{Br}^{opti} \times G_{Br} + [K]_{Bark}^{opti} \times G_{Bark} + [K]_{CR}^{opti} \times G_{CR} + [K]_{FR}^{opti} \times G_{FR} \right) \quad (12)$$

200 where K_{NPP} (gK.m^{-2}) was the quantity of K necessary for optimal stoichiometry of newly formed organ biomass, NPP_{org}
(gC.m^{-2}.day^{-1}) the daily net primary production minus the allocation to the leaves, K_{org}^{opti} (gK.gC^{-1}) the optimal concentra-
tion of the considered organ (eq.15-18) and G_{org} the allocation coefficient of that organ (eq. 2 to 4).

The quantity of available K was a function of K content in the phloem sap and the minimal quantity of K in the phloem sap
(Part 1):

205 $$K_{available} = K_{phloem} - K_{phloem}^{min} \quad (13)$$

where $K_{available}$ (gK.m^{-2}) was the amount of K available for organ growth, K_{phloem} (gK.m^{-2}) the amount of K in the phloem
sap, K_{phloem}^{min} ($gK.m^{-2}$) the minimal amount of K in the phloem sap (see Part 1).

The limitation of K allocation to newly formed organ nutrient content was simply the ratio between available K and K demand:

$$Lim_{org}^{K} = \frac{min\Big(K_{available}, K_{NPP}\Big)}{K_{NPP}} \tag{14}$$

where $K_{available}$ was from eq. 13 and K_{NPP} ($gK.m^{-2}$) the amount of K needed for optimal stoichiometry of newly formed organs (eq.12).

The cycle of K in the leaves is described in Part 1 since it is an integral part of the canopy cohort model.

2.6.1 Wood

Due to the continuous phenology of tropical eucalypt trees, K dynamics in wood were simulated through daily cohorts of wood. This was also the preferred modelling choice since it provided a mechanistic explanation for wood remobilisation throughout wood aging (that we considered to be leaching of K from sapwood into the xylem sap). The trunk NPP was allocated daily to a cohort of wood. In parallel, the optimal K concentration of newly formed wood ($[K]_{Trunk}$) was constant and equal to the maximum trunk concentration measured at the fertilisation experiment (Fig.S5), i.e. the K content of cohort i at its creation was the following:

$$K_{phloem \rightarrow Trunk}^{i} = [K]_{Trunk}^{opti} \times Lim_{org}^{K} \times NPP_{trunk} \tag{15}$$

where $K_{phloem \rightarrow Trunk}^{i}$ ($gK.m^{-2}.day^{-1}$) was the flux of K to the cohort i at the time of its creation, $[K]_{Trunk}^{opti}$ ($gK.gC^{-1}$) the optimal concentration of newly formed wood, Lim_{org}^{K} the limitation by K availability (eq. 14) and NPP_{trunk} ($gC.m^{-2}.day^{-1}$) the daily trunk increment.

Since K concentration of the total trunk tissue decreases with trunk biomass, it was necessary to implement wood K remobilisation in the model. A model where the remobilisation rate was dependent on wood production was the best suited for this task since it showed the best fit with experimental data when compared to a model where remobilisation was independent of wood production. The following equation was used:

$$K_{trunk \rightarrow xylem}^{i} = K_{Trunk}^{i} \times T_{KTrunk} \times NPP_{trunk} \tag{16}$$

where $K_{trunk \rightarrow xylem}^{i}$ ($gK.m^{-2}$) was the remobilisation of K from the cohort i, K_{Trunk}^{i} ($g.m^{-2}$) the K mineralomass of the trunk cohort i, T_{KTrunk} ($.gC^{-1}$) the remobilisation rate per unit of trunk production, and NPP_{trunk} ($gC.m^{-2}.day^{-1}$) the daily trunk increment. Remobilised K was allocated to K_{xylem}. If the K concentration of the cohort ($[K]_{Trunk}^{i}$) was lower than a threshold value $[K]_{Trunk}^{min}$ ($gK.gC^{-1}$), there was no remobilisation ($K_{trunk \rightarrow xylem}^{i} = 0$). The threshold, $[K]_{Trunk}^{min}$, was determined from the minimum asymptot of the relationship between trunk biomass and trunk K concentration at the fertilization experiment (Fig.S5). This measured value was assumed to be the minimum concentration of a cohort since it was assumed that at a high enough wood biomass, the proportion of K associated to newly formed wood to the total wood K content was negligible (Augusto et al., 2000). This meant that the measured concentration of wood as a whole was similar to the minimum concentration of K in the trunk at high enough trunk biomass.

2.6.2 Branches

240 The optimal K concentration of newly formed branches was a function of the branch biomass.

$$[K]_{Br}^{opti} = 0.00707 \times e^{-0.00854 \times B_{Br}} + 0.000759 \tag{17}$$

where $[K]_{Br}^{opti}$ was the K concentration of the newly formed branches in gK.gC^{-1} and B_{Br} was the branch biomass in gC.m^{-2}. This decreasing function was fitted on experimental nutrient content and biomass data collected in the fertilised plots.

Before falling as litter to the ground, branches that die stay attached some months to the tree. Whenever dead branches are
245 mentioned, we mean dead branches still attached to the trunk. During branch death, part of branch K was remobilized into K_{xylem}. The remobilisation efficiency ($R_{KBranch}$, eq.16) was considered constant and was calculated using the difference between dead branch and live branch K concentration in experimental data. The value that was used here was calculated as the remobilisation rate in the first year (Fig.S4). This was done as we assumed that the dead branches that were dosed at that moment had potentially spent less time as dead branches (than dead branches later on in the rotation) and we would minimise
250 the leaching effect. Since we could not know what proportion of the K loss between the living branches and dead branches was due to leaching or remobilisation we assumed that this was the best method to avoid error.

2.6.3 Bark

The optimal K concentration of newly formed bark was a function of the bark biomass.

$$[K]_{Bark}^{opti} = 0.00204 \times e^{-0.0057 \times B_{Bark}} + 0.00147 \tag{18}$$

255 where $[K]_{Bark}^{opti}$ was the K concentration of the newly formed bark in gK.gC^{-1} and B_{Bark} was the bark biomass in gC.m^{-2}. The parameters for this function were fitted on experimental data collected in the fertilised plots. No remobilization was considered for bark since there no measurements were available.

2.6.4 Roots

The optimal K concentration (in gK.gC^{-1}) of coarse ($[K]_{CR}^{opti}$) and fine roots ($[K]_{FR}^{opti}$) was a fixed value independent of tree
260 age or biomass. Due to the absence of data regarding this process, the model did not simulate remobilisation from roots. The K content of dead fine roots was added to the K litter pool, which in turn leached into the soil available K and could be uptaken by other living roots.

2.6.5 Total remobilisation in woody organs

Total remobilisation was the flux of K from the woody organs to the xylem. It was calculated as the following:

265 $$K_{remob} = K_{trunk \rightarrow xylem} + R_{Kbranches} \times K_{branches}^{mortality} \tag{19}$$

where K_{remob} (gK.m^{-2}.day^{-1}) was the total remobilisation flux, $K_{trunk \to xylem}$ (gK.m^{-2}.day^{-1}) the remobilisation rate of wood, $R_{Kbranches}$ the remobilisation rate of dying branches and $K_{branches}^{mortality}$ (gK.m^{-2}.day^{-1}) the flux of K from living branches to dead branches.

2.7 Simulations

270 The simulation initialisations were conducted to resemble as closely as possible the omission experiment. Simulations in the fully fertilised treatment (+K) were initialised with the same fertilisation values as the fertilised control in the experiment (i.e. 17.5 gK m-2) corresponding to a one-time application of fertiliser at planting. Simulations in the K omission treatment (oK) shared the same initialisation except that the fertiliser pool was initialised with 0 gK.

To investigate the effects of a fertilisation gradient, 10 initialisation values of K pools spanning from no input (in oK) to 17.5
275 gK (+K) were chosen.

To test whether the fertilisation regime could have an impact on tree productivity, two fertilisation regimes were simulated. One where the K dose was brought all at once (as in the experiment) and one where the same K fertiliser dose was broken up into 4 sub-doses that were temporally spaced (equivalent to the Eucflux experiment, see Part 1).

2.8 Analysis

280 To test the accuracy of model prediction, the Root Mean Square Errors of simulations' output variables were calculated using measurements at the experimental site. The mean of the 3 experimental blocs (there were 3 blocs per experimental treatment) was used. To normalise this metric and have a relative Root Mean Square Error, the RMSE was divided by the measured mean throughout the rotation of the considered output variable.

To describe the response of resource use efficiency (RUE) to different levels of K availability, we used the following metrics.

285 2.9 Carbon use efficiency

The carbon-use efficiency was calculated as the simulated NPP flux divided by the simulated GPP flux (De Lucia et al., 2007). It is in fact a measure of the proportion of assimilated carbon that was not lost to respiration.

2.9.1 Water use efficiency

The water use efficiencies of NPP (WUE$_{NPP}$) and trunk NPP (WUE$_{trunk}$) were calculated by dividing the total NPP or trunk
290 NPP by the amount of transpired water during the period over which NPP and trunk NPP were calculated.

2.9.2 Potassium use efficiency

Potassium use efficiencies of GPP (KUE$_{GPP}$), total NPP (KUE$_{NPP}$) and trunk NPP (KUE$_{trunk}$) were calculated by dividing the respective C-based metric by the maximum amount of K that was immobilised in the plant during the rotation. For example

in the case of (KUE$_{NPP}$):

$$295 \quad KUE_{NPP} = \frac{\sum_{i=0}^{k} NPP_i}{K_{plant}^{max}} \tag{20}$$

where KUE_{NPP} (gC.gK^{-1}) was the K-use efficiency of total NPP, k the number of days in the rotation (days), NPP (gC.m^{-2}.day^{-1}) the daily NPP of the rotation, and K_{plant}^{max} (gK.m^{-2}) the maximum of K that was immobilized in the plant during the rotation (the maximum of total simulated plant K during the rotation). For calculating KUE$_{GPP}$ and KUE$_{trunk}$ the numerator of the above fraction can be replaced by GPP or NPP$_{trunk}$ respectively. There are many alternative ways to calcu-

300 late nutrient use efficiencies in forests (Turner and Lambert, 2014). Here, we decided to use total K immobilisation instead of uptake since circulation of K in the system was high and we think that the maximum amount of K accumulated in standing biomass is a more relevant representation of total system K demand. Indeed, the maximum K accumulated in standing biomass is a proxy of the amount of K necessary in the system and along the rotation for the plant considering its biomass. In systems where there is less restitution to the soil, it would be equivalent to the soil nutrient uptake.

305 ### 2.9.3 Fertiliser use efficiency

Fertiliser use efficiencies were computed as the difference of cumulated NPP between the simulated K omission stand (oK) and stands simulated with different K fertilisation levels, and dividing it by the amount of K fertiliser added. This allowed us to compute the growth gain in carbon per unit of K fertiliser used:

$$FUE_{NPP}^{f} = \frac{\sum_{i=0}^{k}(NPP_i^f - NPP_i^{oK})}{K_{fertiliser}^{added}} \tag{21}$$

310 where FUE_{NPP}^{f} (gC.gK^{-1}) the fertiliser use efficiency of NPP for a given level of fertilisation, k the number of days in the rotation (days), NPP^f (gC.m^{-2}.day^{-1}) the daily NPP of the currently considered stand, NPP^{oK} (gC.m^{-2}.day^{-1}) the NPP of the K omission stand and $K_{fertiliser}^{added}$ (gK.m^{-2}) the amount of K fertiliser that was added in the considered stand. To obtain FUE_{GPP} or FUE_{Trunk}, this relationship can be applied to either GPP or NPP_{trunk}, respectively.

3 Results

315 ### 3.1 Prediction of changes in NPP caused by GPP

The model was capable of replicating most of the NPP and biomass differences between the +K and oK stands (Fig. 2). In the +K stand, the five-year cumulated GPP, NPP and trunk NPP (NPP$_{trunk}$) were, respectively, 19830 gC.m^{-2} (i.e. 3966 gC.m^{-2}.yr^{-1} on average), 9950 gC.m^{-2} (1990 gC.m^{-2}.yr^{-1}), and 5795 gC.m^{-2} (1159 gC.m^{-2}.yr^{-1}). In the oK stand, they were respectively 8907 gC.m^{-2} (1781 gC.m^{-2}.yr^{-1}), 3578 gC.m^{-2} (715 gC.m^{-2}.yr^{-1}) and 1781 gC.m^{-2} (414

320 gC.m^{-2}.yr^{-1}). The GPP, NPP and NPP$_{trunk}$ were respectively 55%, 64% and 70% lower in the oK stand compared to the +K stand. The reduction in GPP was in line with what was simulated at the Eucflux site (Table 2 of Part 1) and GPP estimations using the TBCA method applied to C stocks and C fluxes measured throughout the rotation in our experiment (not shown,

Giardina and Ryan, 2002). The reduction of trunk NPP_{trunk} was comparable to data (Fig. 2b). The same could be said for the bark (Fig. 2d) and the branches (Fig. 2f). This led to simulated biomasses in line with measurements in the +K and oK stands

325 for branches (Fig. 2e, bark (Fig. 2c) and trunk (Fig. 2a). In the +K stand the RMSEs (and normalised RMSEs in parentheses) for trunk, branches, bark, leaves and total aboveground biomass were respectively: 385 (12%), 50 (17%), 34 (9%), 48 (19%), and 363 $gC.m^{-2}$ (9%). In the oK stand they were respectively: 155 (16%), 48 (37%), 25 (17%), 31 (26%), and 193 $gC.m^{-2}$ (15%). The errors of simulations relative to measured values of total aboveground biomass at age 59 months were an underestimation of 24 $gC.m^{-2}$ (-1%) in the +K stand and an overestimation of 161 $gC.m^{-2}$ (6%) in the oK stand. This overestimation

330 of aboveground biomass was concurrent to an underestimation of root biomass (Fig. 2i).

3.2 Consequences of K addition on C allocation patterns within trees

The model allowed the study of allocation in the trees under different K fertilisation regimes. The simulated allocation patterns did not differ greatly between the fertilised and omission stands (Fig 3a). However, simulated carbon use efficiency (defined as the ratio of NPP to GPP) was reduced by 23% in the omission stand (Fig.S6b, 0.52 vs 0.40). The ratio of wood productivity

335 to GPP (CUE_{trunk}) was reduced by the same proportion (21%) showing that the reduction of NPP_{trunk} followed the same dynamic than total NPP. Moreover the difference in CUE between the two fertilisation treatments increased throughout the rotation (a 2% difference the first year, and a 17% difference the fifth). The trend was similar for CUE_{trunk}. The difference in CUE between the two treatments was mainly due to an increase of maintenance respiration in the oK stand where it accounted for 48% of the GPP compared to 34% in the +K stand. This was further amplified by leaf NPP representing 13% of GPP in oK

340 compared to 7% in +K.

The model was also capable of simulating the response of the different carbon fluxes, along the stand rotation, to a gradient of initial K fertilisation (Fig. 3b). It showed that the responses of GPP, NPP and wood productivity to fertilisation all saturated at around 11 $gK.m^{-2}$ for a five-year rotation. The simulated carbon fluxes did not show any sensitivity to the fertilisation application regime (one or four time application, Fig.S6a). The simulations conducted with the one-time application at planting

345 compared with the same amount of K split in 4 applications at 0, 3, 10, and 20 months of age showed little to no differences in GPP, NPP and NPP_{trunk} (Fig.S6a). The wood productivity was similar in all fertilisation treatments in the first year of the rotation (Fig. 3). This result was in contrast to experimental data that shows that the relative difference in organ NPP appears early the rotation (Laclau et al., 2009). While the response of CUE_{NPP} resembled a linear function before it saturated at a fertilisation of 11 $gK.m^{-2}$, the response of CUE_{trunk} followed a non linear response (Fig.S6b) by increasing from 0 to 2

350 $gK.m^{-2}$ of fertilisation added as KCl fertiliser, saturating between 2 and 4 $gK.m^{-2}$ and increasing linearly between 4 and 11 $gK.m^{-2}$.

3.3 K cycling in the trees

The model showed that the main sinks of K in both the +K and oK stands were the woody organs (trunk, bark and branches). Despite the remobilisation of K in the trunk, the quantity of K immobilised in the trunk increased linearly with time in both

355 treatments (Fig. 4) thus constituting an important K sink.
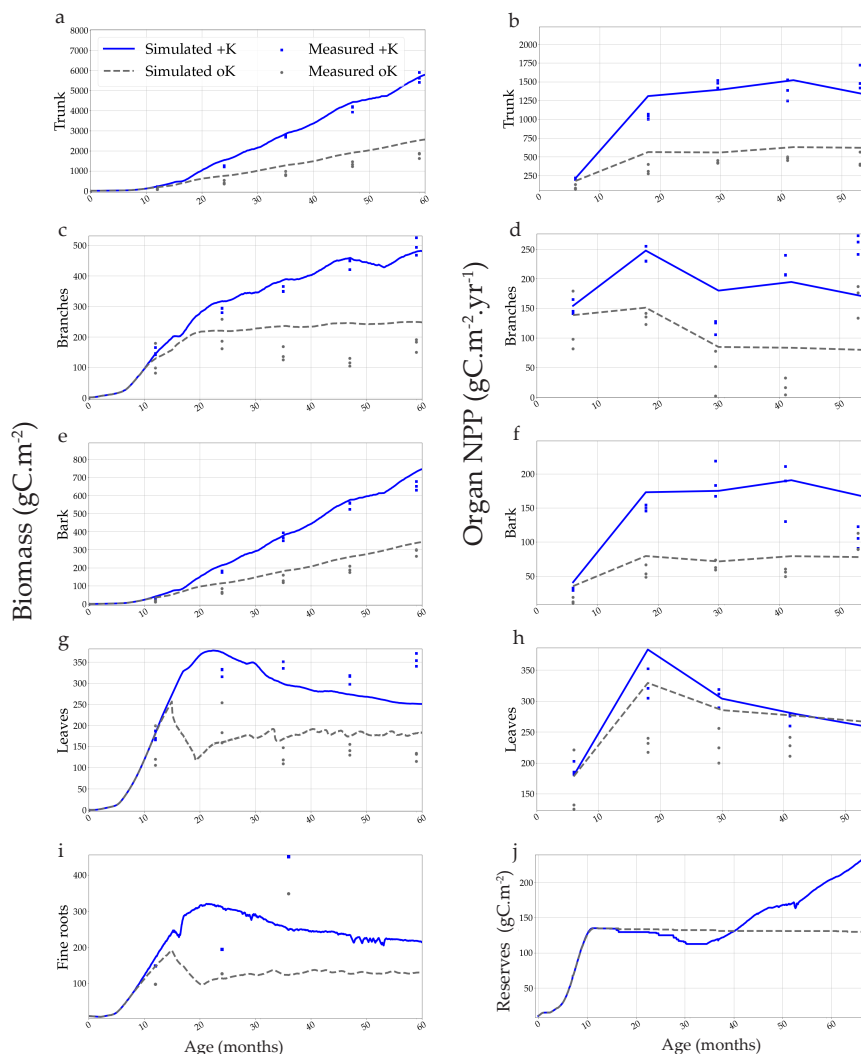
Figure 2. Simulated biomass of the different organs in two contrasted K availability scenarios (no K fertilisation, oK, and full K fertilisation, +K) in: a) trunk, c) bark, e) branches, g) leaves, i) fine roots and j) reserves. On the right column, the respective measured and simulated annual NPP of each organ: b) trunk, d) Bark, f) Branches, h) Leaves.
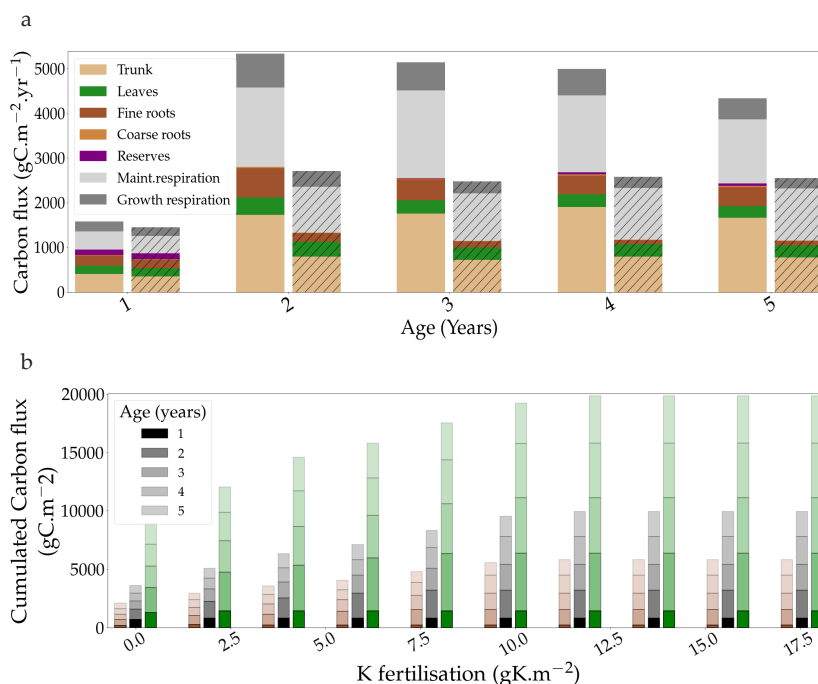
Figure 3. a) The simulated allocation of assimilated carbon to the different organs and respiration fluxes in 2 contrasted fertilisation conditions: +K and oK (hatched). b) The response of simulated carbon fluxes, cumulated over five years, to different fertilisation levels. Total GPP is in green, total NPP in black and trunk NPP in brown.

The theoretical minimum concentration of K in the xylem sap (assuming no recirculating K) of our trees was calculated by dividing the daily simulated flux of K that circulated in the xylem sap (uptake, wood and branch remobilisation) by the simulated transpiration flux of each day. The mean simulated minimum xylem sap K concentration over the course of a rotation was 0.30 mM (0.012 gK.L^{-1}) in the fully fertilised stand and 0.11 mM (0.004 gK.L^{-1}) in the K omission stand. When

360   including the K content of the phloem sap and leaf resorption (which means the total circulating K in the tree) in this calculation, the values were 1.66 mM (0.065 gK.L^{-1}) and 0.46 mM (0.018 gK.L^{-1}), respectively.

The simulation of internal and external K fluxes in the system (Tab. 1) showed that in the fully fertilised and K omission stands, wood remobilisation represented the most important flux of K. Implementing in the model this process of K remobilisation from wood increased the model accuracy substantially (not shown here) by buffering the amount of K available for

365   organ growth. When added to branch and leaf resorption, the total amount of K remobilised represented 1.8 times the K uptake in the fertilised stand versus 1.4 times in the omission stand. In the simulated oK stand, K uptake was very similar to the sum of the litterfall, leaching and atmospheric deposition fluxes, in all but the first year of the rotation (Tab. 1). The deposition flux represented more than 50% of the uptake flux in these K deficient conditions. Moreover, in the K omission stand, an increase of the simulated weathering flux from 0 to 0.3 gK.m^{-2}.yr^{-1} (in the range of possible values, see Cornut et al., 2021) led to an

increase of 23, 28 and 30% of the rotation-cumulated GPP, NPP and NPP$_{trunk}$ respectively. This showed that small differences in K input can lead to big differences in outcome for wood productivity.

The difference in the K flux of canopy leaching between the two simulated stands (much lower in the omission stand, Tab. 1) was in line with results obtained on eucalypt plantations at K-rich and K-deficient sites (Laclau et al., 2010). This was the result of lower leaf K concentration and supports the validity of the leaching model used here (see Part 1).
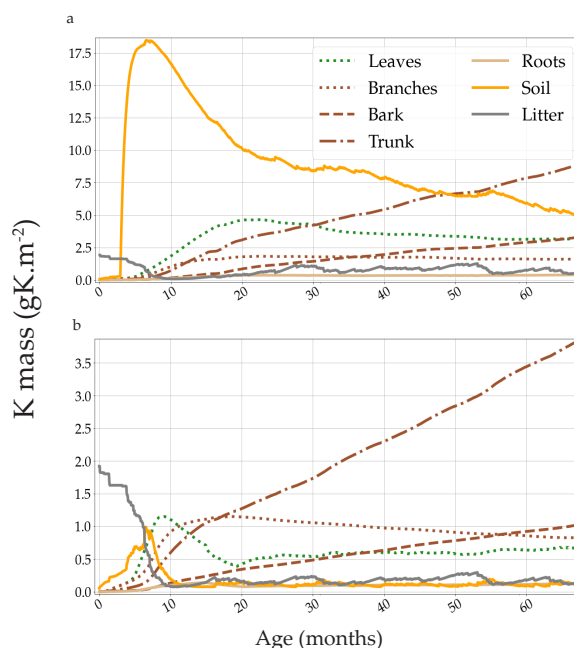
Figure 4. Simulated K mass of all the compartments containing K. Two contrasted K availability scenarios are displayed: a) high fertilisation (+K in the main text), b) no K fertilisation (oK in the main text). Note differences in the y-axis scale.

Age	Wood remob. +K − oK	Branch remob. +K − oK	Leaf resorption +K − oK	Uptake +K − oK	Litterfall +K − oK	Leaching +K − oK
0 → 1	0.35 − 0.19	0.12 − 0.10	0.36 − 0.75	5.61 − 2.90	0.07 − 0.05	0.03 − 0.02
1 → 2	7.71 − 1.13	0.41 − 0.26	1.96 − 0.92	7.39 − 0.96	1.49 − 0.45	0.25 − 0.01
2 → 3	9.21 − 1.13	0.44 − 0.24	2.68 − 0.70	4.39 − 1.00	2.30 − 0.42	0.26 − 0.01
3 → 4	10.01 − 1.19	0.43 − 0.21	2.23 − 0.69	4.39 − 0.92	1.90 − 0.40	0.15 − 0.01
4 → 5	8.73 − 1.12	0.41 − 0.19	2.07 − 0.66	3.86 − 0.99	1.80 − 0.39	0.15 − 0.01

Table 1. Simulated yearly fluxes of K (in gK.m^{-2}.yr^{-1}) in a fully fertilised treatment (+K) and in a K omission treatment (oK). This table contains both internal fluxes (wood, branch and leaf remobilisations) and exchange fluxes (uptake, litterfall and canopy leaching). The constant atmospheric deposition flux (0.5 gK.m^{-2}.yr^{-1}) is not shown.

16

3.4 Water and potassium use efficiencies

Omission of K fertiliser decreased stand transpiration by 51%. The reduction (13%) of simulated GPP water use efficiency (WUE_{GPP}) between the +K (0.0035 $gC_{GPP}.gH_2O^{-1}$) and oK (0.0031 $gC_{GPP}.gH_2O^{-1}$) stands was comparable to results obtained on the Eucflux site in Part 1. On the other hand, simulated WUE_{NPP} showed a much stronger response to K deficiency. The reduction was on the order of 33% with WUE_{NPP} at 0.0018 and 0.0012 $gC.gH_2O^{-1}$ in the +K stand and oK stand respectively. The simulated water use efficiency of trunk wood was also reduced by 32 % in oK relative to +K. The WUE_{trunk} values in the +K and oK stands were respectively 0.0011 and 0.0007 $gC.gH_2O^{-1}$.

In the following paragraph, potassium use efficiency (KUE) is understood as the ratio of a cumulated carbon flux at the end of the rotation and maximum value of K immobilized in the tree. The simulated KUE_{GPP} were 1281 and 1994 $gC.gK_{plant}^{-1}$ in the +K and oK stands, respectively. In contrast, the simulated KUE_{NPP} and KUE_{trunk} only increased by 19% (owing to decreased CUE in the oK stand) between the +K and oK stands. The simulated KUE_{trunk} were 387 and 462 $gC.gK_{Plant}^{-1}$ in the +K and oK stands, respectively (656 and 784 respectively for KUE_{NPP}).

FUE generally decreased with increasing fertilisation (Fig.S7). However, a two-slope relationship was apparent: at low levels of fertilisation, increases in fertilisation led to strong increases in NPP. However, for high amounts of fertiliser applied, wood production per unit of K declined. At intermediate levels of fertilisation (between 6 to 10 $gK.m^2$) the FUE was almost constant or slightly increased. However, at higher levels of initial fertilisation the FUE linearly decreased (consequence of a stable NPP with linearly increasing fertilisation, Fig. 3b).

3.5 Stoichiometry of organs

Potassium concentrations in trunk wood and in branches were correctly simulated (Fig. 5) using a simple limitation of the K flux entering into each organ in function of the organ-specific K optimal concentrations used (Eq.12-18). The mean K concentrations in the total tree biomass were 0.0048 $gK.gDM^{-1}$ in the +K stand and 0.0030 $gK.gDM^{-1}$ in the oK stand. This corresponded to a decrease of 36% of the K concentration in the oK stand relative to the +K stand. This revealed that total plant stoichiometric flexibility was high in the model, which is in accordance with measurements.

The new model of wood growth and K remobilisation was validated by the simulated concentrations that were in line with experimental measurements both in the fully fertilised and in the K omission treatment (Fig. 5a) without the need for additional forcing. However, the simulated concentration of K in branches (Fig. 5b) was overestimated in the oK stand. An important amount of K was also stored in bark and branches in the simulated K omission stand (Fig. 4b) and it was the most important K stock at the beginning of the oK rotation.
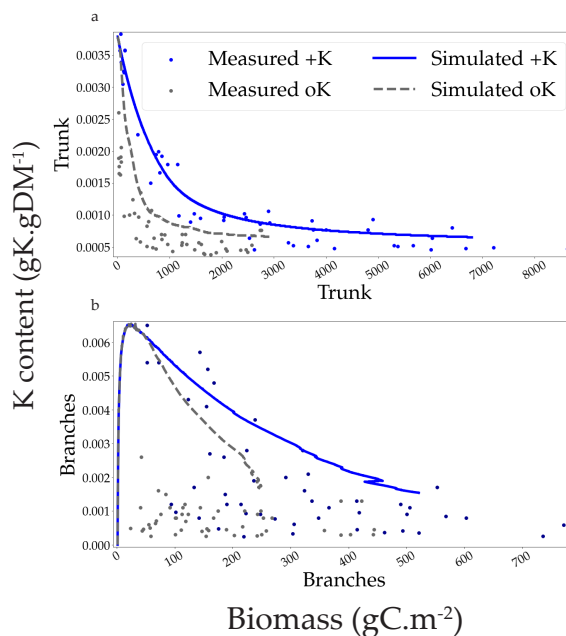
Figure 5. Simulated concentrations of K in stemwood (a) and branches (b) in two contrasted K availability scenarios compared to measurements conducted in the fertilisation experiment at Itatinga.

4 Discussion

4.1 GPP-limitation of NPP and partitioning of photosynthates

405 The CASTANEA-MAESPA-K model was largely successful in reproducing the limitation of wood productivity induced by K deficiency (Fig.2). This makes it the first mechanistic model to simulate the interaction between the K cycle and forest NPP. Combined with the fact that partitioning in the model was not directly impacted by K availability (there was no mechanism through which K directly impacted carbon allocation to wood), which suggests that the limitation of wood productivity in the absence of K fertilisation was mainly due to GPP-limitation. However, the consequences of K deficiency were higher for NPP

410 than for GPP. This was due to a decrease in CUE at low levels of fertilisation. This is similar to the general trend for world forests, which is a decrease forests' biomass production-GPP ratio (a proxy for CUE) with decreasing fertility (Vicca et al., 2012). Here, the partitioning of GPP to the different organs was not strongly affected by K availability (except for leaves going from 7% in +K to 13% of NPP in oK). The reduced CUE was mainly the result of an increased autotrophic respiration in proportion to the biomass of organs mirroring the increase in the ratio of ecosystem respiration to GPP in nutrient-poor forests

415 (Fernández-Martínez et al., 2014). While the relationship between GPP and net ecosystem productivity was not significant for low fertility forest sites in this meta-analysis, this was not the case for GPP and NPP in our study.

Only simulated fine root biomasses were under-estimated in both the +K and oK stands (Fig.2j). This suggests that simulating a root target biomass that is function of leaf area (Marsden et al., 2013) might not be appropriate in this instance (since the shape of the root biomass curve during the rotation is qualitatively different). One other cause could be a misestimation of root lifespan

420 since measurements of fine root turnover have yielded a wide range of values (Jourdan et al., 2008; Lambais et al., 2017). The estimation of fine root turnover had also been an constraint to simulating N mineralisation rates in Australian eucalypt stands with the G'DAY model (Corbeels et al., 2005). The values of GPP that were simulated here (a mean of 3986 gC.m^{-2}.yr^{-1} in +K and 1709 gC.m^{-2}.yr^{-1} in oK) were on the high range of values expected for terrestrial ecosystems (Baldocchi and Penuelas, 2019; Luyssaert et al., 2007), especially considering these values were a 6 year mean that included the first year after

425 planting. They were similar to values estimated using TBCA measurements in highly productive eucalypt plantations (Ryan et al., 2004, 2010) and clonal experiments at the Eucflux site (unpublished data, see Part 1 for the site description).

The K fertilisation level value at which K-limitation was totally alleviated in simulations (Fig.3b) was similar to the 12 gK.m^{-2} of fertilisation that are commonly added to commercial eucalypt plantations in Brazil (Cornut et al., 2021).

4.2   Water and potassium use efficiency is affected by K availability

430 The simulated RUEs of NPP and NPP$_{trunk}$ were strongly affected by K availability (modelled here as a change in fertilisation levels). Variations of WUE$_{trunk}$ are in line with experimental results that showed a decrease in WUE$_{trunk}$ in the K omission stand at the Itatinga site (Battie-Laclau et al., 2016). While simulated WUE$_{trunk}$ was 33% lower in oK than in +K, measurements showed a decrease of 37% (Battie-Laclau et al., 2016). This confirms the relevance of a model-based approach in studying the effect of K availability on WUE$_{trunk}$. However, the model diverged from measurements in the same stands at the

435 end of the stand rotation (from 4 to 6 years after planting) that showed that WUE$_{trunk}$ of the K omission stand was reduced by 75% as compared to the WUE$_{trunk}$ of the +K stand (Asensio et al., 2020), while CASTANEA-MAESPA-K only showed a reduction by 39% of WUE$_{trunk}$ between these two stands at this age. Since the trunk NPP simulated by the model agreed with measurements (Fig.2b) and the model simulated a reduction in transpiration consistent with different approaches (see Part 1), trunk WUE in the oK stand might have been underestimated by the measurements presented in Asensio et al. (2020).

440 Both the changes in KUE and FUE along a K fertilisation gradient showed some interesting results. While K fertilisation strongly decreased KUE for GPP, the effects on NPP and trunk NPP were weaker, as a result of an increase in CUE (Fig.S7). This was a consequence of reduced CUE. FUE results demonstrate that the response of wood productivity is not a linear function of fertilisation and that at low levels of fertilisation, small increases in K fertilisation levels produce a strong increase in NPP. Simulated NPP was maximal with the highest fertilizer amount, however the trend is asymptotical, with more than 95%

445 of trunk NPP (Fig.3b) already reached at around 10 gK.m^{-2}, a value commonly applied in commercial eucalypt plantations managed in this soil type. Partitioning of the K fertilisation in only one or in several amounts did not changed the wood production, considering that no deep leaching occurs in these systems, in agreement with the conclusions of field studies measuring soil solution chemistry in deep soil layers (Laclau et al., 2010).

4.3 Circulation of K in the plant and stoichiometry

450 Our work pinpointed the importance of a plant K circulation model. The total remobilisation flux of K from the branches, the trunk and the leaves was higher than the K uptake in the soil at all fertilisation levels. In C-N (Zaehle et al., 2010; Thum et al., 2019) or C-N-P (Goll et al., 2017) coupled models, stoichiometry of organs can be a direct limiter of organ growth. A strong effect of stoichiometry on soil organic matter decomposition has also been historically used in models of organic matter decomposition in soils (Parton et al., 1988). While such mechanisms were not considered in our modelling approach

455 (organ K concentration is allowed to vary unconstrained), the reduction in NPP was enough to compensate the reduction in K availability such that the simulated stoichiometries of organs do not vary more than they do in the measurements (Fig.S5). The stoichiometric flexibility of trees could be higher for K than for N and P. This is consistent with observations of wood K content, which depends mainly on abiotic conditions while P wood content depends mainly on the species (Bauters et al., 2022). Our model suggests that leaves have a higher stoichiometric flexibility than wood (not shown here), in agreement

460 with observations in a Mediterranean forest environment (Sardans et al., 2012). However, the model failed at reproducing the patterns of stoichiometric plasticity (variability in K concentration of organs) that were observed in between the woody organs, in particular in branches (measurements show high stoichiometric flexibility in branches). This suggests that organs can differ in K homeostasis. The failure of the model to reproduce stoichiometric flexibilities in wood and bark (not shown here) could potentially have had an influence on the amount of K available for leaf expansion thus overestimating the K limitation on

465 canopy surface and leaf functioning. This is further exacerbated by the large amount of K stored in the bark and in the branches in the simulated K omission stand, especially when the model showed a strong K limitation of leaves (between the 10th and 20th month after planting).

The simulated amount of K immobilised in the trunk at the end of the rotation in the +K stand was an order of magnitude lower than what is observed in tropical forests (Bauters et al., 2022). This is due to a low total biomass in planted forests

470 managed in short rotation compared to a natural forest since the simulated K concentrations in the trunk were in the range of values reported in old-growth tropical forests. The yearly increase in the amount of K stored in the trunk was in the range of observed values (see Fig.1 in Bauters et al., 2022) both for the oK and +K stands. This suggests that tropical eucalypt plantations could be a relevant model system for certain parts of the K cycle. The quantity of K that was allocated daily to wood and remobilised gradually (see eq.7), acted as a buffer that prevented an overestimation of K limitation once K in the soil

475 reached very low values. This shows that wood can act as a storage organ for K and can alleviate low uptake of K under drought (Sardans and Peñuelas, 2007; Touche et al., 2022) or in planted forests only fertilised at planting and growing on K-poor soils.

While the K trunk remobilisation fluxes were higher in our model than what was previously calculated using other methods (a mean of 7.6 $gK.m^{-2}.yr^{-1}$ vs 2.7 $gK.m^{-2}.yr^{-1}$ in Sette et al., 2013), the amount of K that transited in the xylem sap every day was low considering the magnitude of the sapflow in the xylem for tree transpiration. This led to very low xylem sap K

480 concentrations if a flux of K from phloem sap to xylem sap was not considered. Since values of xylem sap K concentrations measured on different plants are one order of magnitude higher (Nardini et al., 2010; Siebrecht et al., 2003), our results either suggest that xylem sap K concentrations are very variable between plants or that an intense recirculation of K between xylem

and phloem is taking place. The first hypothesis is consistent with evidence from temperate conifers that show a variation of an order of magnitude (the lower bound is similar to values calculated from our simulations) of xylem sap K concentration during the growing season (Losso et al., 2018). However, the last hypothesis seems more plausible since K is necessary to maintain xylem hydraulic conductivity (Oddo et al., 2011; Nardini et al., 2011) and that considering a transfer of K from phloem sap to xylem sap, the calculated K xylem sap concentrations more in line with measurements from the literature. It also supports evidence that K^+ ions are an essential part of many processes at the plant level (Dreyer and Michard, 2020): energy source (Dreyer et al., 2017), counter-ion for NO_3^-, signaling (Anschütz et al., 2014), protection against abiotic stress (Cakmak, 2005), among others. The intense recirculation of K between xylem and phloem serving as a way to maintain homeostasis. The order of magnitude of this recirculation would have to be determined experimentally. Previous measurements have shown that up to 25% of K^+ ions are recirculated in tomato plants (Armstrong and Kirkby, 1979) and up to 50% in *Ricinus communis* seedlings (Marschnert et al., 1997). Results from our model suggest that the figure could be higher in eucalypt trees (maybe owing to remobilisation from wood absent from tomato plants).

5 Conclusion

The results shown here show the relevance of using a mechanistic model to explore the links between K availability and forest NPP. Our model was able to reproduce results from fertilisation experiments with a good degree of accuracy while also being able to simulate an availability gradient in K. The model allowed us to formulate the following conclusions:

1. The decrease in GPP caused by K deficiency explained most of the difference in wood productivity between K-rich and K-deficient stands. There was no need for a direct modification of the partitioning process or stoichiometric limitations to explain the observed patterns of productivity;

2. Potassium-use efficiency to produce wood increases with diminishing K availability suggesting that the trees are able to compensate for lower K content in tissues, through reduced carbon-use efficiency;

3. The major importance of external inputs (weathering and deposition mainly) already observed in GPP simulations (see Part 1) is also critical for the ecosystem's NPP;

4. The importance of internal K fluxes in the trees that provide buffering against temporally localised K limitations and contributes to explaining why an adequate K supply limited to the early stage of the development of trees can be sufficient to sustain high NPPs over the entire rotation in planted forests growing in highly weathered soils.

References

510 Anschütz, U., Becker, D., and Shabala, S.: Going beyond nutrition: Regulation of potassium homoeostasis as a common denominator of plant adaptive responses to environment, Journal of Plant Physiology, 171, 670–687, https://doi.org/10.1016/j.jplph.2014.01.009, 2014.

Armstrong, M. J. and Kirkby, E. A.: Estimation of Potassium Recirculation in Tomato Plants by Comparison of the Rates of Potassium and Calcium Accumulation in the Tops with Their Fluxes in the Xylem Stream, Plant Physiology, 63, 1143–1148, https://doi.org/10.1104/pp.63.6.1143, 1979.

515 Asensio, V., Domec, J.-C., Nouvellon, Y., Laclau, J.-P., Bouillet, J.-P., Jordan-Meille, L., Lavres, J., Rojas, J. D., Guillemot, J., and Abreu-Junior, C. H.: Potassium fertilization increases hydraulic redistribution and water use efficiency for stemwood production in Eucalyptus grandis plantations, Environmental and Experimental Botany, 176, 104 085, https://doi.org/10.1016/j.envexpbot.2020.104085, 2020.

Augusto, L., Ranger, J., Ponette, Q., and Rapp, M.: Relationships between forest tree species, stand production and stand nutrient amount, Annals of Forest Science, 57, 313–324, https://doi.org/10.1051/forest:2000122, 2000.

520 Baldocchi, D. and Penuelas, J.: The physics and ecology of mining carbon dioxide from the atmosphere by ecosystems, Global Change Biology, 25, 1191–1197, https://doi.org/10.1111/gcb.14559, 2019.

Baribault, T. W., Kobe, R. K., and Finley, A. O.: Tropical tree growth is correlated with soil phosphorus, potassium, and calcium, though not for legumes, Ecological Monographs, 82, 189–203, https://doi.org/10.1890/11-1013.1, 2012.

Battie-Laclau, P., Laclau, J.-P., Piccolo, M. d. C., Arenque, B. C., Beri, C., Mietton, L., Muniz, M. R. A., Jordan-Meille, L., Buckeridge, 525 M. S., Nouvellon, Y., Ranger, J., and Bouillet, J.-P.: Influence of potassium and sodium nutrition on leaf area components in Eucalyptus grandis trees, Plant and Soil, 371, 19–35, https://doi.org/10.1007/s11104-013-1663-7, 2013.

Battie-Laclau, P., Delgado-Rojas, J. S., Christina, M., Nouvellon, Y., Bouillet, J.-P., Piccolo, M. d. C., Moreira, M. Z., Gonçalves, J. L. d. M., Roupsard, O., and Laclau, J.-P.: Potassium fertilization increases water-use efficiency for stem biomass production without affecting intrinsic water-use efficiency in Eucalyptus grandis plantations, Forest Ecology and Management, 364, 77–89, 530 https://doi.org/10.1016/j.foreco.2016.01.004, 2016.

Battie-Laclau, P., Laclau, J.-P., Domec, J.-C., Christina, M., Bouillet, J.-P., Piccolo, M. d. C., Gonçalves, J. L. d. M., Moreira, R. M. e., Krusche, A. V., Bouvet, J.-M., and Nouvellon, Y.: Effects of potassium and sodium supply on drought-adaptive mechanisms in Eucalyptus grandis plantations, New Phytologist, 203, 401–413, https://doi.org/10.1111/nph.12810, 2014.

Bauters, M., Grau, O., Doetterl, S., Heineman, K. D., Dalling, J. W., Prada, C. M., Griepentrog, M., Malhi, Y., Riutta, T., Scalon, M., Oliveras, 535 I., Inagawa, T., Majalap, N., Beeckman, H., Van den Bulcke, J., Perring, M. P., Dourdain, A., Hérault, B., Vermeir, P., Makelele, I. A., Fernández, P. R., Sardans, J., Peñuelas, J., and Janssens, I. A.: Tropical wood stores substantial amounts of nutrients, but we have limited understanding why, Biotropica, p. btp.13069, https://doi.org/10.1111/btp.13069, 2022.

Cakmak, I.: The role of potassium in alleviating detrimental effects of abiotic stresses in plants, Journal of Plant Nutrition and Soil Science, 168, 521–530, https://doi.org/10.1002/jpln.200420485, 2005.

540 Cakmak, I., Hengeler, C., and Marschner, H.: Changes in phloem export of sucrose in leaves in response to phosphorus, potassium and magnesium deficiency in bean plants, Journal of Experimental Botany, 45, 1251–1257, https://doi.org/10.1093/jxb/45.9.1251, 1994.

Christina, M., Laclau, J.-P., Gonçalves, J. L. M., Jourdan, C., Nouvellon, Y., and Bouillet, J.-P.: Almost symmetrical vertical growth rates above and below ground in one of the world's most productive forests, Ecosphere, 2, art27, https://doi.org/10.1890/ES10-00158.1, 2011.

Christina, M., Maire, G. L., Battie-Laclau, P., Nouvellon, Y., Bouillet, J.-P., Jourdan, C., Gonçalves, J. L. d. M., and Laclau, J.-P.: Mea-
545   sured and modeled interactive effects of potassium deficiency and water deficit on gross primary productivity and light-use efficiency in
       Eucalyptus grandis plantations, Global Change Biology, 21, 2022–2039, https://doi.org/10.1111/gcb.12817, 2015.

Christina, M., Nouvellon, Y., Laclau, J.-P., Stape, J. L., Bouillet, J.-P., Lambais, G. R., and Maire, G. l.: Importance of deep water uptake in
       tropical eucalypt forest, Functional Ecology, 31, 509–519, https://doi.org/10.1111/1365-2435.12727, 2017.

Christina, M., le Maire, G., Nouvellon, Y., Vezy, R., Bordon, B., Battie-Laclau, P., Gonçalves, J. L. M., Delgado-Rojas, J. S.,
550   Bouillet, J. P., and Laclau, J. P.: Simulating the effects of different potassium and water supply regimes on soil water content
       and water table depth over a rotation of a tropical Eucalyptus grandis plantation, Forest Ecology and Management, 418, 4–14,
       https://doi.org/10.1016/j.foreco.2017.12.048, 2018.

Corbeels, M., McMurtrie, R. E., Pepper, D. A., and O'Connell, A. M.: A process-based model of nitrogen cycling in forest plantations: Part
       II. Simulating growth and nitrogen mineralisation of Eucalyptus globulus plantations in south-western Australia, Ecological Modelling,
555   187, 449–474, https://doi.org/10.1016/j.ecolmodel.2005.07.004, 2005.

Cornut, I., Le Maire, G., Laclau, J.-P., Guillemot, J., Mareschal, L., Nouvellon, Y., and Delpierre, N.: Potassium limitation of wood pro-
       ductivity: A review of elementary processes and ways forward to modelling illustrated by Eucalyptus plantations, Forest Ecology and
       Management, 494, 119 275, https://doi.org/10.1016/j.foreco.2021.119275, 2021.

De Lucia, E. H., Drake, J. E., Thomas, R. B., and Gonzalez-Meler, M.: Forest carbon use efficiency: is respiration a constant fraction of gross
560   primary production?, Global Change Biology, 13, 1157–1167, https://doi.org/10.1111/j.1365-2486.2007.01365.x, 2007.

Doman, D. C. and Geiger, D. R.: Effect of Exogenously Supplied Foliar Potassium on Phloem Loading in Beta vulgaris L., Plant Physiology,
       64, 528–533, https://doi.org/10.1104/pp.64.4.528, 1979.

Dreyer, I. and Michard, E.: High- and Low-Affinity Transport in Plants From a Thermodynamic Point of View, Frontiers in Plant Science,
       10, https://doi.org/10.3389/fpls.2019.01797, 2020.

565   Dreyer, I., Gomez-Porras, J. L., and Riedelsberger, J.: The potassium battery: a mobile energy source for transport processes in plant vascular
       tissues, New Phytologist, 216, 1049–1053, https://doi.org/10.1111/nph.14667, 2017.

Dufrêne, E., Davi, H., François, C., Maire, G. l., Dantec, V. L., and Granier, A.: Modelling carbon and water cycles in
       a beech forest: Part I: Model description and uncertainty analysis on modelled NEE, Ecological Modelling, 185, 407–436,
       https://doi.org/10.1016/j.ecolmodel.2005.01.004, 2005.

570   Duursma, R. A. and Medlyn, B. E.: MAESPA : a model to study interactions between water limitation, environmental drivers and vegetation
       function at tree and stand levels, with an example application to [CO2] x drought interactions, Geoscientific model development, pp.
       919–940, https://doi.org/10.5194/gmd-5-919-2012, 2012.

Epron, D., Laclau, J.-P., Almeida, J. C. R., Gonçalves, J. L. M., Ponton, S., Sette, C. R., Delgado-Rojas, J. S., Bouillet, J.-P., and Nouvellon, Y.:
       Do changes in carbon allocation account for the growth response to potassium and sodium applications in tropical Eucalyptus plantations?,
575   Tree Physiology, 32, 667–679, https://doi.org/10.1093/treephys/tpr107, 2012.

Epron, D., Cabral, O. M. R., Laclau, J.-P., Dannoura, M., Packer, A. P., Plain, C., Battie-Laclau, P., Moreira, M. Z., Trivelin, P.
       C. O., Bouillet, J.-P., Gérant, D., and Nouvellon, Y.: In situ 13CO2 pulse labelling of field-grown eucalypt trees revealed the ef-
       fects of potassium nutrition and throughfall exclusion on phloem transport of photosynthetic carbon, Tree Physiology, 36, 6–21,
       https://doi.org/10.1093/treephys/tpv090, 2016.

580 Fernández-Martínez, M., Vicca, S., Janssens, I. A., Sardans, J., Luyssaert, S., Campioli, M., Chapin III, F. S., Ciais, P., Malhi, Y., Obersteiner, M., Papale, D., Piao, S. L., Reichstein, M., Rodà, F., and Peñuelas, J.: Nutrient availability as the key regulator of global forest carbon balance, Nature Climate Change, 4, 471–476, https://doi.org/10.1038/nclimate2177, 2014.

Gazola, R. d. N., Buzetti, S., Teixeira Filho, M. C. M., Gazola, R. P. D., Celestrino, T. d. S., Silva, A. C. d., Silva, P. H. M. d., Gazola, R. d. N., Buzetti, S., Teixeira Filho, M. C. M., Gazola, R. P. D., Celestrino, T. d. S., Silva, A. C. d., and Silva, P. H.
585 M. d.: Potassium Fertilization of Eucalyptus in an Entisol in Low-Elevation Cerrado, Revista Brasileira de Ciência do Solo, 43, https://doi.org/10.1590/18069657rbcs20180085, 2019.

Giardina, C. P. and Ryan, M. G.: Total Belowground Carbon Allocation in a Fast-growing Eucalyptus Plantation Estimated Using a Carbon Balance Approach, Ecosystems, 5, 487–499, https://doi.org/10.1007/s10021-002-0130-8, 2002.

Goll, D., Vuichard, N., Maignan, F., Jornet-Puig, A., Sardans, J., Violette, A., Peng, S., Sun, Y., Kvakic, M., Guimberteau, M., Guenet, B.,
590 Zaehle, S., Peñuelas, J., Janssens, I., and Ciais, P.: A representation of the phosphorus cycle for ORCHIDEE (revision 4520), Geosci. Model Dev., p. 27, 2017.

Gonçalves, J. L. d. M.: Nutrição e fertilização florestal, IPEF, 2000.

Jourdan, C., Silva, E. V., Gonçalves, J. L. M., Ranger, J., Moreira, R. M., and Laclau, J. P.: Fine root production and turnover in Brazilian Eucalyptus plantations under contrasting nitrogen fertilization regimes, Forest Ecology and Management, 256, 396–404,
595 https://doi.org/10.1016/j.foreco.2008.04.034, 2008.

Laclau, J.-P., Almeida, J. C. R., Gonçalves, J. L. M., Saint-André, L., Ventura, M., Ranger, J., Moreira, R. M., and Nouvellon, Y.: Influence of nitrogen and potassium fertilization on leaf lifespan and allocation of above-ground growth in Eucalyptus plantations, Tree Physiology, 29, 111–124, https://doi.org/10.1093/treephys/tpn010, 2009.

Laclau, J.-P., Ranger, J., de Moraes Gonçalves, J. L., Maquère, V., Krusche, A. V., M'Bou, A. T., Nouvellon, Y., Saint-André, L., Bouillet,
600 J.-P., de Cassia Piccolo, M., and Deleporte, P.: Biogeochemical cycles of nutrients in tropical Eucalyptus plantations, Forest Ecology and Management, 259, 1771–1785, https://doi.org/10.1016/j.foreco.2009.06.010, 2010.

Lambais, G. R., Jourdan, C., de Cássia Piccolo, M., Germon, A., Pinheiro, R. C., Nouvellon, Y., Stape, J. L., Campoe, O. C., Robin, A., Bouillet, J.-P., le Maire, G., and Laclau, J.-P.: Contrasting phenology of Eucalyptus grandis fine roots in upper and very deep soil layers in Brazil, Plant and Soil, 421, 301–318, https://doi.org/10.1007/s11104-017-3460-1, 2017.

605 Lockhart, J. A.: An analysis of irreversible plant cell elongation, Journal of Theoretical Biology, 8, 264–275, https://doi.org/10.1016/0022-5193(65)90077-9, 1965.

Losso, A., Nardini, A., Dämon, B., and Mayr, S.: Xylem sap chemistry: seasonal changes in timberline conifers Pinus cembra, Picea abies, and Larix decidua, Biologia plantarum, 62, 157–165, https://doi.org/10.1007/s10535-017-0755-2, 2018.

Luyssaert, S., Inglima, I., Jung, M., Richardson, A. D., Reichstein, M., Papale, D., Piao, S. L., Schulze, E.-D., Wingate, L., Matteucci, G.,
610 Aragao, L., Aubinet, M., Beer, C., Bernhofer, C., Black, K. G., Bonal, D., Bonnefond, J.-M., Chambers, J., Ciais, P., Cook, B., Davis, K. J., Dolman, A. J., Gielen, B., Goulden, M., Grace, J., Granier, A., Grelle, A., Griffis, T., Grünwald, T., Guidolotti, G., Hanson, P. J., Harding, R., Hollinger, D. Y., Hutyra, L. R., Kolari, P., Kruijt, B., Kutsch, W., Lagergren, F., Laurila, T., Law, B. E., Maire, G. L., Lindroth, A., Loustau, D., Malhi, Y., Mateus, J., Migliavacca, M., Misson, L., Montagnani, L., Moncrieff, J., Moors, E., Munger, J. W., Nikinmaa, E., Ollinger, S. V., Pita, G., Rebmann, C., Roupsard, O., Saigusa, N., Sanz, M. J., Seufert, G., Sierra, C., Smith, M.-L., Tang, J., Valentini,
615 R., Vesala, T., and Janssens, I. A.: CO2 balance of boreal, temperate, and tropical forests derived from a global database, Global Change Biology, 13, 2509–2537, https://doi.org/10.1111/j.1365-2486.2007.01439.x, 2007.

Marschner, H., Kirkby, E. A., and Cakmak, I.: Effect of mineral nutritional status on shoot—root partitioning of photoassimilates and cycling of mineral nutrients, Journal of Experimental Botany, 47, 1255–1263, https://www.jstor.org/stable/23695325, 1996.

Marschnert, H., Kirkby, E. A., and Engels, C.: Importance of Cycling and Recycling of Mineral Nutrients within Plants for Growth and
620   Development, Botanica Acta, 110, 265–273, https://doi.org/10.1111/j.1438-8677.1997.tb00639.x, 1997.

Marsden, C., Nouvellon, Y., Laclau, J.-P., Corbeels, M., McMurtrie, R. E., Stape, J. L., Epron, D., and le Maire, G.: Modifying the G'DAY process-based model to simulate the spatial variability of Eucalyptus plantation growth on deep tropical soils, Forest Ecology and Management, 301, 112–128, https://doi.org/10.1016/j.foreco.2012.10.039, 2013.

Muller, B., Pantin, F., Génard, M., Turc, O., Freixes, S., Piques, M., and Gibon, Y.: Water deficits uncouple growth from photosynthesis,
625   increase C content, and modify the relationships between C and growth in sink organs, Journal of Experimental Botany, 62, 1715–1729, https://doi.org/10.1093/jxb/erq438, 2011.

Nardini, A., Grego, F., Trifilò, P., and Salleo, S.: Changes of xylem sap ionic content and stem hydraulics in response to irradiance in Laurus nobilis, Tree Physiology, 30, 628–635, https://doi.org/10.1093/treephys/tpq017, 2010.

Nardini, A., Salleo, S., and Jansen, S.: More than just a vulnerable pipeline: xylem physiology in the light of ion-mediated regulation of plant
630   water transport, Journal of Experimental Botany, 62, 4701–4718, https://doi.org/10.1093/jxb/err208, 2011.

Oddo, E., Inzerillo, S., La Bella, F., Grisafi, F., Salleo, S., Nardini, A., and Goldstein, G.: Short-term effects of potassium fertilization on the hydraulic conductance of Laurus nobilis L., Tree Physiology, 31, 131–138, https://doi.org/10.1093/treephys/tpq115, 2011.

Pantin, F., Simonneau, T., and Muller, B.: Coming of leaf age: control of growth by hydraulics and metabolics during leaf ontogeny, New Phytologist, 196, 349–366, https://doi.org/10.1111/j.1469-8137.2012.04273.x, 2012.

635 Parton, W. J., Stewart, J. W. B., and Cole, C. V.: Dynamics of C, N, P and S in grassland soils: a model, Biogeochemistry, 5, 109–131, https://doi.org/10.1007/BF02180320, 1988.

Rocha, J. H. T., Gonçalves, J. L. d. M., Ferraz, A. d. V., Poiati, D. A., Arthur Junior, J. C., and Hubner, A.: Growth dynamics and productivity of an Eucalyptus grandis plantation under omission of N, P, K Ca and Mg over two crop rotation, Forest Ecology and Management, 447, 158–168, https://doi.org/10.1016/j.foreco.2019.05.060, 2019.

640 Ryan, M. G., Binkley, D., Fownes, J. H., Giardina, C. P., and Senock, R. S.: An Experimental Test of the Causes of Forest Growth Decline with Stand Age, Ecological Monographs, 74, 393–414, https://doi.org/10.1890/03-4037, 2004.

Ryan, M. G., Cavaleri, M. A., Almeida, A. C., Penchel, R., Senock, R. S., and Luiz Stape, J.: Wood CO2 efflux and foliar respiration for Eucalyptus in Hawaii and Brazil, Tree Physiology, 29, 1213–1222, https://doi.org/10.1093/treephys/tpp059, 2009.

Ryan, M. G., Stape, J. L., Binkley, D., Fonseca, S., Loos, R. A., Takahashi, E. N., Silva, C. R., Silva, S. R., Hakamada, R. E., Ferreira, J. M.,
645   Lima, A. M. N., Gava, J. L., Leite, F. P., Andrade, H. B., Alves, J. M., and Silva, G. G. C.: Factors controlling Eucalyptus productivity: How water availability and stand structure alter production and carbon allocation, Forest Ecology and Management, 259, 1695–1703, https://doi.org/10.1016/j.foreco.2010.01.013, 2010.

Sardans, J. and Peñuelas, J.: Drought changes phosphorus and potassium accumulation patterns in an evergreen Mediterranean forest, Functional Ecology, 21, 191–201, https://doi.org/10.1111/j.1365-2435.2007.01247.x, 2007.

650 Sardans, J. and Peñuelas, J.: Potassium: a neglected nutrient in global change: Potassium stoichiometry and global change, Global Ecology and Biogeography, 24, 261–275, https://doi.org/10.1111/geb.12259, 2015.

Sardans, J., Peñuelas, J., Coll, M., Vayreda, J., and Rivas-Ubach, A.: Stoichiometry of potassium is largely determined by water availability and growth in Catalonian forests, Functional Ecology, 26, 1077–1089, https://doi.org/10.1111/j.1365-2435.2012.02023.x, 2012.

Sette, C. R., Laclau, J.-P., Tomazello Filho, M., Moreira, R. M., Bouillet, J.-P., Ranger, J., and Almeida, J. C. R.: Source-driven remobi-
655   lizations of nutrients within stem wood in Eucalyptusgrandis plantations, Trees, 27, 827–839, https://doi.org/10.1007/s00468-012-0837-x,
       2013.

Siebrecht, S., Herdel, K., Schurr, U., and Tischner, R.: Nutrient translocation in the xylem of poplar ? diurnal variations and spatial distribution
       along the shoot axis, Planta, 217, 783–793, https://doi.org/10.1007/s00425-003-1041-4, 2003.

Thum, T., Caldararu, S., Engel, J., Kern, M., Pallandt, M., Schnur, R., Yu, L., and Zaehle, S.: A new model of the coupled carbon, nitrogen,
660   and phosphorus cycles in the terrestrial biosphere (QUINCY v1.0; revision 1996), Geoscientific Model Development, 12, 4781–4802,
       https://doi.org/10.5194/gmd-12-4781-2019, 2019.

Touche, J., Calvaruso, C., De Donato, P., and Turpault, M.: Five successive years of rainfall exclusion induce nutritional stress in a mature
       beech stand, Forest Ecology and Management, 507, 119 987, https://doi.org/10.1016/j.foreco.2021.119987, 2022.

Tripler, C. E., Kaushal, S. S., Likens, G. E., and Walter, M. T.: Patterns in potassium dynamics in forest ecosystems, Ecology Letters, 9,
665   451–466, https://doi.org/10.1111/j.1461-0248.2006.00891.x, 2006.

Turner, J. and Lambert, M. J.: Analysis of nutrient use efficiency (NUE) in Eucalyptus pilularis forests, Australian Journal of Botany, 62,
       558, https://doi.org/10.1071/BT14162, 2014.

Vicca, S., Luyssaert, S., Peñuelas, J., Campioli, M., Chapin III, F. S., Ciais, P., Heinemeyer, A., Högberg, P., Kutsch, W. L., Law, B. E.,
       Malhi, Y., Papale, D., Piao, S. L., Reichstein, M., Schulze, E. D., and Janssens, I. A.: Fertile forests produce biomass more efficiently,
670   Ecology Letters, 15, 520–526, https://doi.org/10.1111/j.1461-0248.2012.01775.x, 2012.

Zaehle, S., Friend, A. D., Friedlingstein, P., Dentener, F., Peylin, P., and Schulz, M.: Carbon and nitrogen cycle dynamics in the O-
       CN land surface model: 2. Role of the nitrogen cycle in the historical terrestrial carbon balance, Global Biogeochemical Cycles, 24,
       https://doi.org/10.1029/2009GB003522, 2010.

Author contributions.   IC carried out the devloment of the model as well as wrote the original draft of the manuscript. ND and GlM supervised
675 the work, participated in the conceptualization of the model and reviewed the original draft of the manuscript. JPL, YN, JG participated in the
acquisiton of the data and reviewed the original draft of the manuscript. All authors provided critical feedback and helped shape the research,
analysis and manuscript.

Competing interests.   The contact author has declared that none of the authors has any competing interests.

Data availability.   Data is not freely available due to private funding of experimental sites but is available upon request.